

The angular momentum transport by the strato-rotational instability in simulated Taylor-Couette flows

A. Brandenburg¹ and G. Rüdiger²

¹ NORDITA, Blegdamsvej 17, DK-2100 Copenhagen Ø, Denmark

² Astrophysikalisches Institut Potsdam, An der Sternwarte 16, D-14482 Potsdam, Germany

November 10, 2018

ABSTRACT

Aims. To investigate the stability and angular momentum transport by the strato-rotational instability in the nonlinear regime.

Methods. The hydrodynamic compressible equations are solved in a cartesian box in which the outer cylinder is embedded. Gravity along the rotation axis leads to density stratification. No-slip boundary conditions are used in the radial direction, while free-slip conditions are used on the two ends of the cylinders.

Results. The strato-rotational instability is confirmed and the Reynolds stress is shown to transport angular momentum away from the axis. However, the growth rate decreases with increasing Reynolds number. This, as well as the presence of boundaries renders this instability less relevant for astrophysical applications.

Key words. Shear flow instability – Accretion disks

1. Introduction

The magneto-rotational instability (MRI) is now commonly invoked in order to explain the origin of turbulence in accretion discs (Balbus & Hawley 1998). This is because there exists no purely hydrodynamic local instabilities in accretion discs in the sense that periodic shearing box calculations do not yield instability. Already when vertical shear is included, there is a linear instability, but for thin discs its growth rate is small compared with that of the MRI (Urpin & Brandenburg 1998; Arlt & Urpin 2004). Purely hydrodynamic instabilities are of interest for protostellar discs where the conductivity is usually so poor that magnetic effects are unimportant, and hence the MRI may be irrelevant. Another possibility for a hydrodynamic instability is the nonlinear shear instability (Chagelishvili et al. 2003, Afshordi, Mukhopadhyay & Narayan 2005). The general difficulty with such models has been discussed by Balbus, Hawley & Stone (1996). However, a conclusive resolution of this problem using simulations remains difficult because of the large Reynolds numbers required.

In an attempt to address the possibility of hydrodynamic instabilities in accretion discs, one can resort to experiments. All these experiments have boundaries, so their relevance to accretion discs is questionable. Nevertheless, such experiments remain interesting in their own right. The possibility of a nonlinear instability of a Taylor-Couette flow experiments has recently been addressed by

Richard & Zahn (1999). The issue was revived by recent findings of Molemaker, McWilliams & Yavneh (2001) who found the possibility of a *linear* instability in Taylor-Couette flow with density stratification along the axis. Dubrulle et al. (2005) confirmed this instability for a range of different radial boundary conditions.

More recent work by Shalybkov & Rüdiger (2005), who considered regular Taylor-Couette flow in the presence of no-slip boundaries, gave a detailed stability criterion for the instability, which is henceforth referred to as the strato-rotational instability (SRI). Withjack & Chen (1974) observed nonaxisymmetric patterns in density-stratified Taylor-Couette flows close and beyond the Rayleigh line.

Umurhan (2005) shows that, within the framework of the quasi-hydrostatic semi-geostrophic approximation, the instability only survives in the presence of no-slip radial boundaries. The purpose of the present paper is to demonstrate the existence of this instability using direct simulations and to calculate its saturation level in the nonlinear regime. In contrast to nonlinear instabilities, the SRI can be studied conveniently by simulations, because the critical Reynolds numbers are well below 10^3 . We are thus also able to compute sign and, in the nonlinear regime, also the amount of angular momentum transport due to the SRI. Let us emphasize here that the sign of angular momentum transport (inwards or outwards) is nontrivial.

There are several examples in the literature (mostly for rotating convection) where the cross correlation

$$Q_{r\phi} = \overline{u'_r u'_\phi} \quad (1)$$

of the one-point correlation tensor

$$Q_{ij} = \overline{u'_i(x, t) u'_j(x, t)} \quad (2)$$

turns out to be negative, i.e. angular momentum is transported inwards by the rotating turbulence (see Ryu & Goodman 1992; Kley, Papaloizou & Lin 1993; Stone & Balbus 1996). The primes in (1) and (2) denote the departures from the toroidally averaged flow, i.e. $\mathbf{u}' = \mathbf{u} - \overline{\mathbf{u}}$, where

$$\overline{\mathbf{u}} = \int_0^{2\pi} \mathbf{u} \, d\phi / 2\pi. \quad (3)$$

Here we shall find that the zonal flux of angular momentum, (1), always proves to be positive i.e. the angular momentum is transported outwards by the SRI.

2. The model

We consider the governing equations for a compressible perfect gas,

$$\frac{D \ln \rho}{Dt} = -\nabla \cdot \mathbf{u}, \quad (4)$$

$$\frac{D \mathbf{u}}{Dt} = \mathbf{g} - c_s^2 (\nabla \ln \rho + \nabla s/c_p) + \mathbf{F}_{\text{visc}} + \mathbf{F}_{\text{rot}} + \mathbf{F}_{\text{drive}}, \quad (5)$$

$$\rho T \frac{Ds}{Dt} = \nabla \cdot (c_p \rho \chi \nabla T), \quad (6)$$

where \mathbf{u} is the velocity, ρ the density, s the specific entropy, $\mathbf{g} = \text{const}$ is gravity, c_p and c_v are the specific heats at constant pressure and volume, respectively, $\gamma = c_p/c_v = 5/3$ is their assumed ratio, c_s is the sound speed, T is the temperature, and the two are related to the other quantities via

$$(\gamma - 1)c_p T = c_s^2 = c_{s0}^2 \exp [\gamma s/c_p + (\gamma - 1) \ln \rho/\rho_0]. \quad (7)$$

Here, c_{s0} and ρ_0 are normalization constants. These constants also define the zero point of the specific entropy. The viscous force is

$$\mathbf{F}_{\text{visc}} = \nu (\nabla^2 \mathbf{u} + \frac{1}{3} \nabla \nabla \cdot \mathbf{u} + 2 \mathbf{S} \cdot \nabla \ln \rho), \quad (8)$$

where $\mathbf{S}_{ij} = \frac{1}{2}(u_{i,j} + u_{j,i}) - \frac{1}{3} \delta_{ij} \nabla \cdot \mathbf{u}$ is the traceless rate of strain tensor, where commas denote partial differentiation. We consider a rotating frame of reference, such that in that frame the angular velocity of the outer cylinder is zero. The resulting apparent force is

$$\mathbf{F}_{\text{rot}} = -2\Omega_{\text{out}} \times \mathbf{u} + \Omega_{\text{out}}^2 \boldsymbol{\varpi}, \quad (9)$$

where $\boldsymbol{\varpi} = (x, y, 0)$ is the cylindrical radius vector. In our frame of reference, the angular velocities of the outer and inner cylinders are imposed by a body force of the form

$$\mathbf{F}_{\text{drive}} = -\tau^{-1} [(\mathbf{u} - \mathbf{u}_{\text{in}}) \xi_{\text{in}}(\mathbf{r}) + \mathbf{u} \xi_{\text{out}}(\mathbf{r})]. \quad (10)$$

where $\xi_{\text{in}}(\mathbf{r}) = 1$ when $|\mathbf{r}| < R_{\text{in}}$ and 0 otherwise, and $\xi_{\text{out}}(\mathbf{r}) = 1$ when $|\mathbf{r}| > R_{\text{out}}$ and 0 otherwise, τ is a relaxation time (comparable to the time step), and $\mathbf{u}_{\text{in}} = (\Omega_{\text{in}} - \Omega_{\text{out}}) \times \mathbf{r}$ is the linear velocity of the inner cylinder in the rotating frame. The temperature is given by $c_p T = c_s^2 / (\gamma - 1)$. Gravity is written as $\mathbf{g} = (0, 0, -g)$, where the value of g is varied.

The *initial* stratification is isothermal ($c_s = c_{s0} = \text{const}$) with $\ln \rho = -z/H$ and $s/c_p = (\gamma - 1)z/H$, where $H = c_{s0}^2 / (\gamma g)$ is the density scale height. The Brunt-Väisälä frequency N is given by

$$N^2 = \frac{g}{c_p} \frac{ds}{dz} = (\gamma - 1) \frac{g^2}{c_s^2} = \left(1 - \frac{1}{\gamma}\right) \frac{g}{H}, \quad (11)$$

which, following Shalybkov & Rüdiger (2005), is expressed in terms of the Froude number, $\text{Fr} = \Omega_{\text{in}}/N$. For $\gamma = 5/3$ and $g = 1$ we have $N = 0.27 \Omega_{\text{in}}$, so $\text{Fr} = 3.7$.

Viscosity and thermal diffusivity are specified in terms of Reynolds and Prandtl numbers,

$$\text{Re} = \Omega_{\text{in}} R_{\text{in}} (R_{\text{out}} - R_{\text{in}})/\nu, \quad \text{Pr} = \nu/\chi, \quad (12)$$

respectively. In all cases considered below we assume $\text{Pr} = 10$, i.e. thermal diffusion is small compared with viscosity. (We need to keep a certain minimum amount of thermal diffusivity to stabilize the code.)

We assume the radial boundaries to be insulating, i.e. $\partial T / \partial \varpi = 0$, and for the velocity we adopt a no-slip boundary condition, i.e.

$$\mathbf{u} = \mathbf{u}_{\text{in}} \quad (\text{on } |\mathbf{r}| = R_{\text{in}}), \quad \mathbf{u} = 0 \quad (\text{on } |\mathbf{r}| = R_{\text{out}}). \quad (13)$$

In the vertical direction we adopt insulating free-slip boundary conditions. The vertical extent of the cylindrical shell is in all cases $L_z = 4$. It is convenient to normalize the various quantities with respect to their values on the inner cylinder and to introduce the ratios

$$\hat{\eta} \equiv R_{\text{in}}/R_{\text{out}}, \quad \hat{\mu} \equiv \Omega_{\text{out}}/\Omega_{\text{in}}. \quad (14)$$

Following Shalybkov & Rüdiger (2005), the flow is strato-rotationally unstable when

$$\hat{\eta}^2 < \hat{\mu} < \hat{\eta} \quad (\text{SRI, nonaxisymmetric}). \quad (15)$$

For $\hat{\mu} < \hat{\eta}^2$ the flow is always Rayleigh unstable both to axisymmetric and to nonaxisymmetric perturbations. In the following we consider the cases $\hat{\eta} = 0.5$ and 0.25 ($R_{\text{out}} = 2$ and 4 , using $R_{\text{in}} = 1$), so we expect the SRI to occur in the ranges $0.25 < \hat{\mu} < 0.5$ and $0.06 < \hat{\mu} < 0.25$ in the two cases. For $\hat{\mu} < 0.25$ (or 0.06) the flow is Rayleigh-unstable.

For the runs presented below the maximum flow speed is at the most 1.2 in units where $\Omega_{\text{in}} = R_{\text{in}} = 1$. In order that the flow remains everywhere subsonic, i.e. $\max(|\mathbf{u}|) < c_s$, we choose $c_{s0} = 3$, which means that the sound speed varies around 3. For the SRI compressibility is however not essential.

We model the problem by embedding the cylinder into a box where the velocities corresponding to rigid

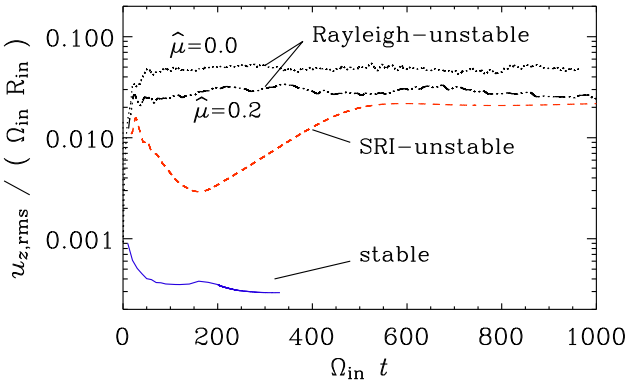


Fig. 1. Amplitudes for $\hat{\mu} = 0, 0.2, 0.3$, and 0.6 . Here, $g/(R_{\text{in}}\Omega_{\text{in}}^2) = 1$ and $\text{Re} = 500$.

inner and outer cylinders is prescribed (see Dobler, Shukurov & Brandenburg 2002 for details regarding this approach). We solve the equations in cartesian geometry using the Pencil Code¹, which is a memory-efficient sixth-order finite difference code using the 2N-RK3 scheme of Williamson (1980). For most of the cases we consider a Reynolds number of 500 where a resolution of 128^3 meshpoints is sufficient. In a few cases we considered larger Reynolds numbers where a higher resolution of up to 512^3 meshpoints was used.

3. Results

3.1. Dependence on $\hat{\mu}$

As a simple diagnostics of the instability we use the root mean square velocity, $u_{z,\text{rms}}$. In Fig. 1 we plot the evolution of $u_{z,\text{rms}}$ for different values of $\hat{\mu}$. As expected, no instability is found for $\hat{\mu} = 0.6$. For smaller values ($\hat{\mu} = 0$ and 0.2), the flow is Rayleigh unstable. For $\hat{\mu} = 0.3$ the flow is strato-rotationally unstable (Fig. 1). Since such flows are stable to axisymmetric perturbations by the Solberg-Høiland criteria (Rüdiger, Arlt & Shalybkov 2002), the instability must be necessarily nonaxisymmetric, which is indeed the case².

3.2. Dependence on g

For weak stratification (small values of g) the growth rate of the instability is small. For small gap width, $\text{Re} = 500$ and $g/R_{\text{in}}\Omega_{\text{in}}^2 = 2$ we find the largest rms velocity. For $g/R_{\text{in}}\Omega_{\text{in}}^2 = 5$ the growth rate is maximum while for $g = 10$ no instability is found; see Fig. 2. However, when Re is increased to 1000, also the case with $g = 10$ yields instability. The number of azimuthal cells increases as the value of g is increased; see Fig. 3, where we show the velocity

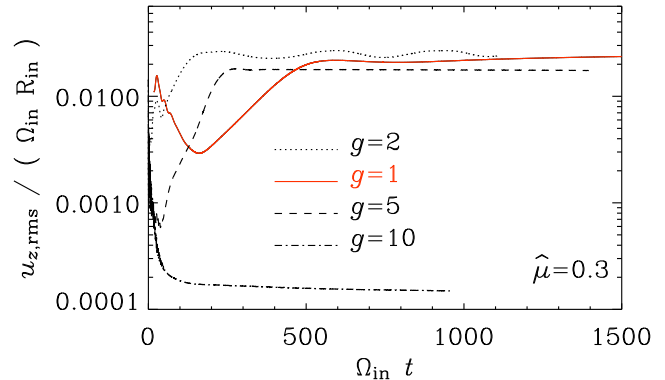


Fig. 2. Amplitudes for $g/(R_{\text{in}}\Omega_{\text{in}}^2) = 1, 2, 5$, and 10 , using $\hat{\mu} = 0.3$ and $\text{Re} = 500$.

field in a meridional cross-section. Note that for $g = 5$ there are 4 eddies in the z direction. Since $L_z/R_{\text{in}} = 4$, the vertical wavelength is 1.

3.3. Critical Reynolds number

The growth rates are on the order of $(0.01\ldots0.02) \times \Omega_{\text{in}}$, which is relatively small. The dependence of the growth rate λ on the Reynolds number Re is shown in Fig. 4. For $\text{Re} < 400$ the vertical rms velocity seems to grow in an oscillatory fashion. However, for $\text{Re} > 500$, the growth rate decreases with increasing Reynolds number.

3.4. Reynolds stress

In order to estimate the ability of the flow to transport angular momentum, we compute the radial component of the Reynolds stress. It turns out that $Q_{r\phi}$ is positive throughout most of the domain, so the flow is transporting angular momentum outwards. The normalized stress, $Q_{r\phi}/(R_{\text{in}}^2\Omega_{\text{in}}^2)$ is around 5×10^{-4} for $g/(R_{\text{in}}\Omega_{\text{in}}^2)$ around 2 and 5. For smaller values of g , the vertical scale of the eddies becomes comparable to or exceeds the vertical extent of the cylinders, so the SRI begins to be suppressed. Likewise, for larger values of g , the vertical scale of the eddies becomes comparable to the scale where viscosity effects can still be regarded as weak.

The fact that the ratio $Q_{r\phi}/(R_{\text{in}}^2\Omega_{\text{in}}^2)$ is much less than unity suggests that angular momentum transport is relatively inefficient. This supplements the earlier impression based on the small value of the normalized growth rate of the instability.

Let us now express the Reynolds stress in astrophysically relevant terms by normalizing it with respect to $H_{\text{in}}^2\Omega_{\text{in}}^2$, where we have chosen the inner radius as reference. (We note that in accretion discs, $H_{\text{in}}\Omega_{\text{in}}$ is proportional to the sound speed.) The Reynolds stress norm

¹ <http://www.nordita.dk/software/pencil-code>

² Animations of the flow, showing also the nonaxisymmetric nature of the instability, can be found on <http://www.nordita.dk/~brandenb/movies/couette/>

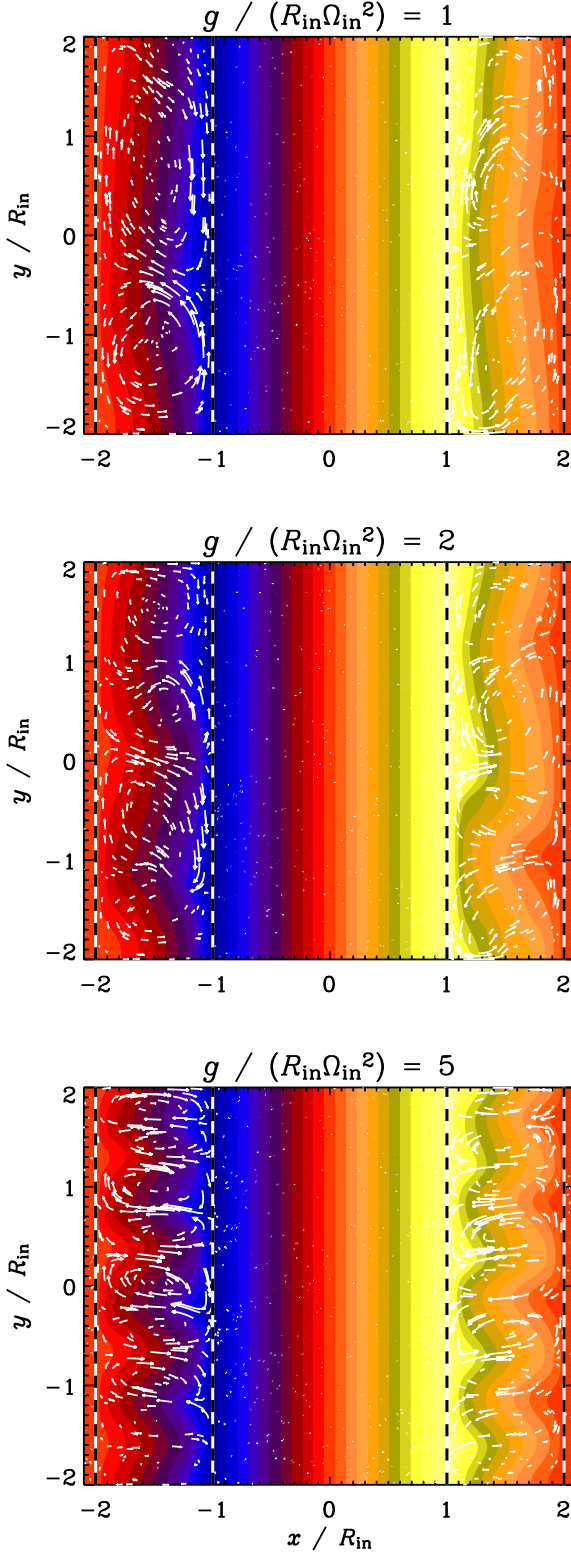


Fig. 3. Velocity pattern in the meridional plane for different values of $g / (R_{\text{in}} \Omega_{\text{in}}^2)$ and $\text{Re} = 500$.

malized in this way is referred to as the Shakura-Sunyaev alpha,

$$\alpha_{\text{SS}} = Q_{r\phi} / (H_{\text{in}}^2 \Omega_{\text{in}}^2). \quad (16)$$

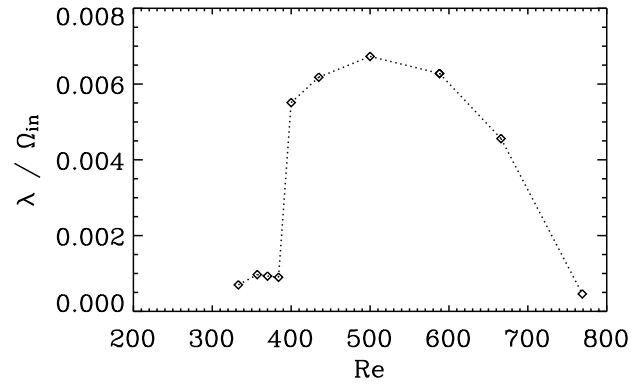


Fig. 4. Dependence of the growth rate λ on the Reynolds number Re . The critical value is about $\text{Re} \approx 400$. For $\text{Re} > 500$, λ decreases with increasing Re .

Table 1. Dependence of the Reynolds stress on gravity for container with small gap.

$g / (R_{\text{in}} \Omega_{\text{in}}^2)$	$Q_{r\phi} / (10^{-4} R_{\text{in}}^2 \Omega_{\text{in}}^2)$	$Q_{zz} / (10^{-4} R_{\text{in}}^2 \Omega_{\text{in}}^2)$
0.5	> 0.16	> 0.04
1	0.9	4.6
2	4.3	5.4
5	4.2	1.1

Table 2. Dependence of the Reynolds stress on gravity for the container with large gap. Note that for $g / (R_{\text{in}} \Omega_{\text{in}}^2) = 2$ the perturbations are slowly decaying.

$g / (R_{\text{in}} \Omega_{\text{in}}^2)$	$Q_{r\phi} / (10^{-4} R_{\text{in}}^2 \Omega_{\text{in}}^2)$	$Q_{zz} / (10^{-4} R_{\text{in}}^2 \Omega_{\text{in}}^2)$
2	0.1	0.02
5	3	0.6

Using the data from Table 1, we find

$$\alpha_{\text{SS}} = (1 \dots 5) \times 10^{-4} (H_{\text{in}} / R_{\text{in}})^{-2}. \quad (17)$$

One may be tempted to insert here the standard result for Shakura-Sunyaev discs, $H/R = 0.03$, which would suggest rather large values of the stress normalized in this way; $\alpha_{\text{SS}} = 0.1 \dots 0.5$. However, this argument assumes that the instability survives for small values of H/R , which is unfortunately not true. Furthermore, for larger radial the instability seems to develop only near the inner cylinder; see Fig. 5. Nevertheless, provided the flow is unstable, the resulting normalized stress, $Q_{r\phi} / (R_{\text{in}}^2 \Omega_{\text{in}}^2)$, is still roughly the same.

4. Conclusions

In the present work we have explored the nonlinear saturation of the strato-rotational instability using a finite difference method. We verify the stability criterion of the

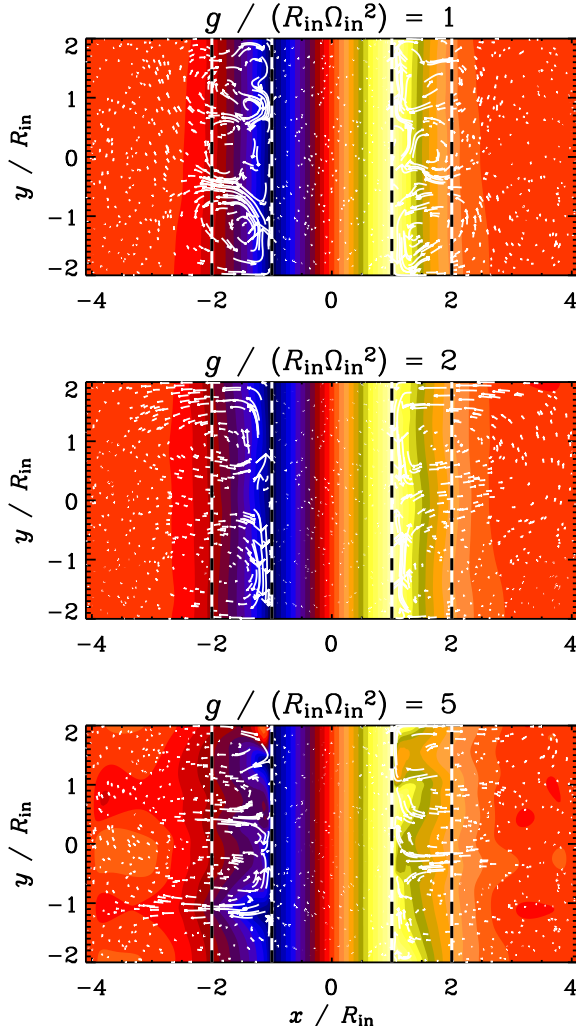


Fig. 5. Velocity pattern in the meridional plane for different values of $g/(R_{\text{in}}\Omega_{\text{in}}^2)$. (For $g/(R_{\text{in}}\Omega_{\text{in}}^2) \leq 2$ the perturbations are slowly decaying.)

Taylor-Couette flow in the presence of vertical stratification. In agreement with earlier results by Shalybkov & Rüdiger (2005), a nonaxisymmetric instability is found when the azimuthal velocity on the inner cylinder, $R_{\text{in}}\Omega_{\text{in}}$, exceeds that on the outer cylinder, $R_{\text{out}}\Omega_{\text{out}}$. This leads to instability in a regime that would be stable by the Solberg-Høiland criteria, which only apply to axisymmetric flows on in the tight-winding approximation (Rüdiger, Arlt & Shalybkov 2002).

Increasing Re sufficiently beyond the critical value for the instability, the growth rate decreases with increasing Re . This is related to the fact that the flow is driven via the viscous force, which is obviously not relevant in astrophysics, but it is relevant to the experiments that are currently being designed to address these questions that are astrophysically motivated in other ways.

Acknowledgements. We thank the organizers and participants of the program ‘‘Magnetohydrodynamics of Stellar Interiors’’ at the Isaac Newton Institute in Cambridge (UK) for a stimulating environment that led to the present work. The Danish

Center for Scientific Computing is acknowledged for granting time on the Linux cluster in Odense (Horseshoe).

References

Afshordi, N., Mukhopadhyay, B., & Narayan, R. 2005, *ApJ*, 629, 373
 Arlt, R., & Urpin, V. 2004, *A&A*, 426, 755
 Balbus, S.A., & Hawley, J.F. 1998, *Rev. Mod. Phys.*, 70, 1
 Balbus, S.A., Hawley, J.F., & Stone, J.M. 1996, *ApJ*, 467, 76
 Chagelishvili, G.D., Zahn, J.-P., Tevzadze, A.G., & Lominadze, J.G. 2003, *A&A*, 402, 401
 Dobler, W., Shukurov, A., & Brandenburg, A. 2002, *PRE*, 65, 036311
 Dubrulle, B., Marie, L., Normand, Ch., Richard, D., Hersant, F., & Zahn, J.-P. 2005, *A&A*, 429, 1
 Kley, W., Papaloizou, J.C.B., & Lin, D.N.C. 1993, *ApJ*, 416, 679
 Molemaker, M.J., McWilliams, J.C., & Yavneh, I. 2001, *PRL*, 86, 5270
 Richard, D., & Zahn, J.-P. 1999, *A&A*, 347, 734
 Rüdiger, G., Arlt, R., & Shalybkov, D. 2002, *A&A*, 391, 781
 Ryu, D., & Goodman, J. 1992, *ApJ*, 388, 438
 Shalybkov, D., & Rüdiger, G. 2005, *A&A*, 438, 411
 Stone, J. M., & Balbus, S. A. 1996, *ApJ*, 464, 364
 Umurhan, O. M. 2005, *MNRAS*, 365, 85
 Urpin, V., & Brandenburg, A. 1998, *MNRAS*, 294, 399
 Williamson, J. H. 1980, *J. Comput. Phys.*, 35, 48
 Withjack, E. M., & Chen, C. F. 1974, *J. Fluid Mech.*, 66, 725